Asymptotic Theory of Bending-Torsion Flutter of High Aspect Ratio Wing in the Torsion Controlled Domain

Gabriel Karpouzian*
United States Naval Academy, Annapolis, Maryland 21402

Abstract

An asymptotic theory of bending-torsion flutter of a high aspect ratio wing with a unit-order bending-torsion stiffness ratio is developed. Two distinct (high and low) frequency domains are identified. For illustration, detailed analysis is carried out only in the high-frequency domain. The methodology is general and may be applicable to various wing configurations. To substantiate its adequacy, the classical case of a uniform unswept cantilever wing in an incompressible airflow is treated as a case study. The asymptotic results for flutter eigenvalues and mode shapes compare favorably with those obtained by a more exact treatment.

Contents

For homogeneous isotropic material, adoption of the Bernoulli-Euler beam deformation model leads to the following governing equations of the coupled bending-torsion wing vibration in a uniform airstream:[1]

$$(EIw_{yy})_{yy} + mw_{tt} - mx_\alpha\theta_{tt} = L_{\text{sec}} \tag{1a}$$

$$-(GJ\theta_y)_y + I_\alpha\theta_{tt} - mx_\alpha w_{tt} = M_{\text{EA}} \tag{1b}$$

where $w(y,t)$ and $\theta(y,t)$ measure the bending and torsion deflections, respectively (Fig. 1). The subscripts y and t indicate partial differentiation, and refer to the spanwise coordinate that coincides with the elastic axis (EA) and the time, respectively. $x_\alpha(y)$ is the downstream distance between the center of mass and the elastic axis at any section; $m(y)$ and $I_\alpha(y)$ are the section mass and section mass moment of inertia (about EA) per unit span; L_{sec} and M_{EA} denote the section lift (positive upward) and section moment about EA (positive nose up) per unit span, respectively. EI and GJ are the sectional bending and torsional stiffnesses. All section properties described above correspond to sections normal to EA. The boundary conditions for a cantilever wing are

$$w = w_y = \theta = 0, \qquad y = 0 \tag{2a}$$

$$w_{yy} = w_{yyy} = \theta_y = 0, \qquad y = b \tag{2b}$$

where b is the wing half-span.

The natural frequencies of a vibrating beam in pure bending and pure torsion have magnitudes proportional to $\omega_B \equiv [EI(0)/m(0)b^4]^{1/2}$ and $\omega_T \equiv [GJ(0)/I_\alpha(0)b^2]^{1/2}$, respectively. Of significance is their ratio

$$\frac{\omega_B}{\omega_T} = \left(\frac{EI(0)}{GJ(0)}\right)^{1/2} \frac{r_\alpha}{AR} \tag{3}$$

where $r_\alpha \equiv 2[I_\alpha(0)/m(0)c(0)^2]^{1/2}$ is the normalized radius of gyration and assumed to be of unit order. $c(0)$ is the root chord length and $AR \equiv 2b/c(0)$ is the wing aspect ratio. Equation (3) indicates that the order of magnitude of ω_B/ω_T is AR^{-1} for a unit-order stiffness ratio. Therefore, two distinct frequency domains can be identified for a high aspect ratio wing ($\omega_B/\omega_T \ll 1$): the torsion-controlled domain (domain I) where $\omega = \mathcal{O}(\omega_T)$, and the bending-dominated domain (domain II) where $\omega = \mathcal{O}(\omega_B)$; ω being the frequency of the coupled mode. This distinct feature of the two domains is merely an asymptotic result which identifies the existence of two distinct frequency scales (high and low), leading to two distinct solution structures. The present analysis is carried out in domain I. A similar analysis has also been developed for domain II.[2]

The local stiffness, inertia, and geometric parameters can be normalized by their respective values at the wing root. The independent variables y and t are normalized by the half-span b and frequency ω, respectively, and the bending displacement w and the twist θ as $h \equiv w/c(0)$ and $\alpha \equiv r_\alpha\theta/2$.

Using the strip theory for the airload and considering harmonic oscillations for flutter of frequency ω, the normalized governing equations, Eqs. (1), and their boundary conditions, Eqs. (2), for a uniform unswept cantilever wing reduce to

$$\hat{\alpha}'' + D\hat{\alpha} - E\hat{h} = 0 \tag{4a}$$

$$\epsilon^2\hat{h}^{\text{IV}} + B\hat{h} + C\hat{\alpha} = 0 \tag{4b}$$

$$\hat{\alpha}(0) = \hat{h}(0) = \hat{h}'(0) = \hat{\alpha}'(1) = \hat{h}''(1) = \hat{h}'''(1) = 0 \tag{5}$$

where $\epsilon \equiv AR^{-1}$ and the symbol "^" denotes the complex amplitudes of the oscillatory modes. The complex constants B, C, D, and E which represent the aerodynamic, structural, and inertia parameters are all of unit order.

The system (4) and (5) represents a singular perturbation problem. There is a breakdown of the solution at the root and tip when $\epsilon \to 0$ since all the boundary conditions cannot be satisfied. The extent of the nonuniformity in these (inner) regions is of order $AR^{-1/2}$, which is used to rescale the problem and obtain asymptotic expansions for the inner solutions by enforcing the boundary conditions in each region. Away from

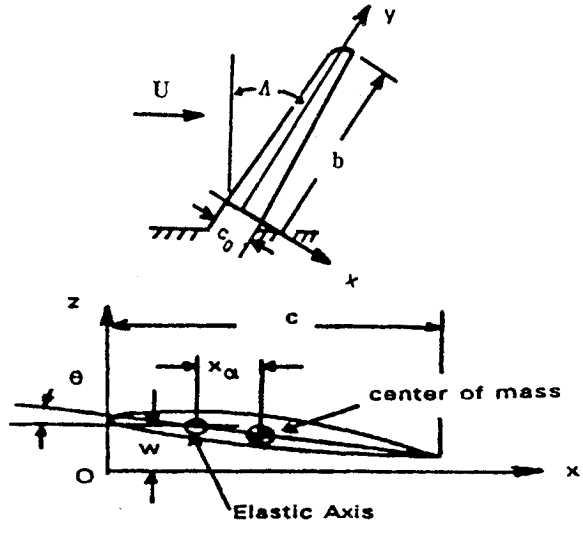

Fig. 1 Swept wing and airfoil configuration.

Received June 22, 1989; revision received Jan. 19, 1990.

*Assistant Professor, Aerospace Engineering Department.

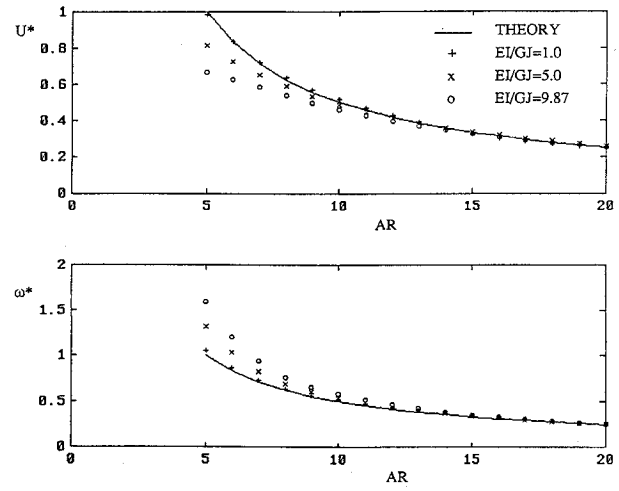

Fig. 2 Comparison of the asymptotic and exact fundamental flutter speed and frequency normalized by the corresponding asymptotic values of $AR = 5$.

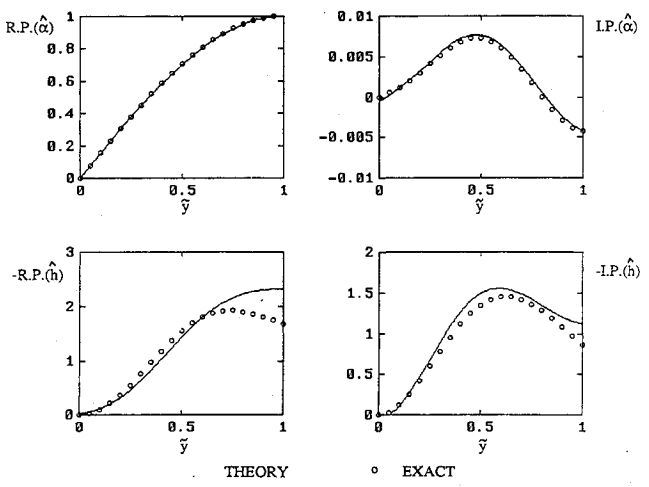

Fig. 3 Comparison of the asymptotic and exact bending-torsion fundamental flutter mode shapes for $AR = 20$ and $EI/GJ = 1$.

the root and tip where the boundary conditions cannot be implemented, asymptotic expansions for the eigenvalues and mode shapes of the (outer) problem are obtained. By applying the method of matched asymptotic expansions, the uniform asymptotic solutions for the torsion and bending mode shapes from root to tip are obtained as

$$\hat{\alpha} = \sin\lambda_0\tilde{y} + \epsilon^{3/2}\left[\lambda_1(\tilde{y}-1)\cos\lambda_0\tilde{y} + \frac{CE\lambda_0}{B(s_2-s_3)}\left(\frac{e^{s2\xi}}{s_2^2}-\frac{e^{s3\xi}}{s_3^2}\right)\right] + \epsilon^2 E\left(\frac{D_2}{s_2^2}e^{s2\eta}+\frac{D_3}{s_3^2}e^{s3\eta}\right)+\ldots \tag{6a}$$

$$\hat{h} = -\frac{C}{B}\sin\lambda_0\tilde{y} + \epsilon^{1/2}\frac{C\lambda_0}{B(s_2-s_3)}(e^{s2\xi}-e^{s3\xi}) + \epsilon(D_2e^{s2\eta}+D_3e^{s3\eta}) + \epsilon^{3/2}\left[\frac{C}{B}\lambda_1(1-\tilde{y})\cos\lambda_0\tilde{y} + \frac{C^2E\lambda_0}{4B^2(s_2-s_3)}\xi\left[\frac{e^{s2\xi}}{s_2}-\frac{e^{s3\xi}}{s_3}\right]+C_2e^{s2\xi}+C_3e^{s3\xi}\right] + \epsilon^2\left[\frac{C\lambda_1}{B(s_2-s_3)}\left(e^{s2\xi}-e^{s3\xi}\right)+\frac{CE}{4B}\eta\left(\frac{D_2}{s_2}e^{s2\eta}+\frac{D_3}{s_3}e^{s3\eta}\right) + E_2e^{s2\eta}+E_3e^{s3\eta}\right]+\cdots \tag{6b}$$

where $\tilde{y} \equiv y/b$ is the outer variable. $\xi \equiv \tilde{y}\epsilon^{-1/2}$ and $\eta \equiv (1-\tilde{y})\epsilon^{-1/2}$ are the inner variables in the root and tip regions. s_2 and s_3 are the complex roots of $s^4 + B = 0$ with negative real parts, and λ_0 and λ_1 are the coefficients of the expansion of the eigenvalue. The constants C_2, C_3, D_2, D_3, E_2, and E_3 can be found from matching conditions.[2]

Results

In order to validate these asymptotic results, we shall compare them with those obtained by the exact method of Ref. 3 for the bending-torsion flutter of a uniform cantilever unswept wing. The wing data in Ref. 3 are $EI = 4.93\times10^5$ $N\text{-}m^2$, $GJ = 0.499\times10^5$ $N\text{-}m^2$, $m = 1.805$ kg/m, $I_\alpha = 0.437$ kg-m^2/m, $x_\alpha = 0.183$ m, $c = 1.83$ m, and $b = 6.1$ m, giving $AR = 6.66$ and $EI/GJ = 9.87$. These data are used for comparison, except for changes in EI and b to reflect the changes in different assigned values of EI/GJ and AR.

Figure 2 compares the results for the flutter speed and frequency in the leading-order approximation with those calculated by the method of Ref. 3 for the fundamental mode as functions of AR. The improvement with increasing AR is apparent.

The torsion and bending flutter mode shapes given by Eqs. (6) are compared with those obtained by the exact calculation for the fundamental mode. Figure 3 shows these comparisons for $AR = 20$ and $EI/GJ = 1$ where the modes are normalized such that $\hat{\alpha}(1) = 1$. We find an excellent agreement for the torsion mode shapes. However, the comparison for the bending mode reveals a discrepancy in the tip region. This discrepancy exists mainly because the number of terms in the asymptotic expansion of the bending mode is not sufficient enough to obtain a high accuracy. Note that, with the same number of terms, the asymptotic results for the torsion mode, Eq. (6a), are excellent, as shown in Fig. 3, because the equation of the bending mode, Eq. (4b), is stiffer than that of the torsion mode, Eq. (4a). Therefore, more terms would be needed in the asymptotic expansion for the bending mode shape, Eq. (6b), to increase its accuracy in the tip region. Equivalently, keeping the same number of terms in the expansion of the bending mode and decreasing the magnitude of the perturbation parameter ϵ, i.e., increasing AR, would yield higher accuracy. In passing, we note that the tip solution may not be as important for other types of wing configuration, such as elliptic or tapered wings, where the tip region is narrower and its effect weaker than that of a rectangular wing.

Acknowledgment

The author is grateful for the support provided by the Naval Academy Research Council.

References

[1]Bisplinghoff, R. L., Ashley, H., and Halfman, R. L. *Aeroelasticity*, Addison-Wesley, Inc., Cambridge, MA, 1955, pp. 102–106.

[2]Cheng, H. K., and Karpouzian, G., "High Aspect Ratio Wing Flutter," University of Southern California, Los Angeles, CA, Report USCAE 142, 1986.

[3]Goland, M., "The Flutter of a Uniform Cantilever Wing," *Journal of Applied Mechanics*, Vol. 12, No. 4, Dec. 1945, pp. 198–208.